Lateral-transfer recirculating etalon spectrometer

Mark A. Stephen,[1,*] Michael A. Krainak,[2] and Molly E. Fahey[2]

[1]*Instrument Systems and Technology Division, NASA's Goddard Space Flight Center, 8800 Greenbelt Road, Greenbelt, MD 20771, USA*

[2]*Laser and Electro-Optics Branch, NASA's Goddard Space Flight Center, 8800 Greenbelt Road, Greenbelt, MD 20771, USA*

[*]*mark.a.stephen@nasa.gov*

Abstract: We describe a Fabry-Perot etalon spectrometer with a novel light recirculation scheme to generate simultaneous parallel wavelength channels with no moving parts. This design uses very simple optics to recirculate light reflected from near normal incidence from the etalon at successively higher angles of incidence. The spectrometer has the full resolution of a Fabry-Perot with significantly improved photon efficiency in a compact, simple design with no moving parts. We present results from a conceptual prototype and a corresponding model.

©2015 Optical Society of America

OCIS codes: (300.0300) Spectroscopy; (280.0280) Remote sensing and sensors; (060.4230) Multiplexing; (120.6200) Spectrometers and spectroscopic instrumentation; (230.7408) Wavelength filtering devices; (280.3640) Lidar.

References and links

1. J. M. Vaughan, *The Fabry-Perot Interferometer: History, Theory, Practice, and Applications* (CRC, 1989).
2. P. Jacquinot, "The luminosity of spectrometers with prisms, gratings, or Fabry-Perot etalons," J. Opt. Soc. Am. **44**(10), 761–765 (1954).
3. G. G. Shepherd, C. W. Lake, J. R. Miller, and L. L. Cogger, "A spatial spectral scanning technique for the Fabry-Perot spectrometer," Appl. Opt. **4**(3), 267–272 (1965).
4. E. Hecht, *Optics* (Addison, Wesley, Longman, 1998).
5. S. Xiao, A. M. Weiner, and C. Lin, "An eight-channel hyperfine wavelength demultiplexer using a Virtually Imaged Phased-Array (VIPA)," IEEE Photonics Technol. Lett. **17**(2), 372–374 (2005).
6. G. Scarcelli and S. H. Yun, "Confocal Brillouin microscopy for three-dimensional mechanical imaging," Nat. Photonics **2**(1), 39–43 (2008).
7. D. E. Jennings and R. J. Boyle, "Multichannel Fabry-Perot spectrometer for infrared astronomy," Appl. Opt. **25**(24), 4520–4522 (1986).
8. M. Mayor, C. Lovis, and N. C. Santos, "Doppler spectroscopy as a path to the detection of Earth-like planets," Nature **513**(7518), 328–335 (2014).
9. M. R. Bowman, A. J. Gibson, and M. C. Sandford, "Atmospheric sodium measured by a tuned laser radar," Nature **221**(5179), 456–457 (1969).
10. C. L. Korb, B. M. Gentry, and S. X. Li, "Edge technique Doppler lidar wind measurements with high vertical resolution," Appl. Opt. **36**(24), 5976–5983 (1997).

1. Introduction

The scanning Fabry-Perot etalon spectrometer [1, 2] is a ubiquitous tool for high-resolution optical spectroscopy. In the most common configuration, the optical path length between the etalon mirrors is (thermally or mechanically) scanned through resonant optical wavelengths that are transmitted in time sequential order. Another common option is to tune the angle of incidence at which the light impinges on the etalon to change the passband [3]. Very high-resolution wavelength measurements can be achieved using etalons. Etalons can be used as tunable filters where the tuning is accomplished by either angle or optical path length changes. By continuously tuning these parameters, one can use an etalon as a high-resolution spectrometer. Figure 1 shows the wavelength and angular dependence on transmission of an etalon (like the one used in our experiment – parameters listed in section 3.)

#249469 Received 3 Sep 2015; revised 2 Nov 2015; accepted 3 Nov 2015; published 6 Nov 2015
© 2015 OSA

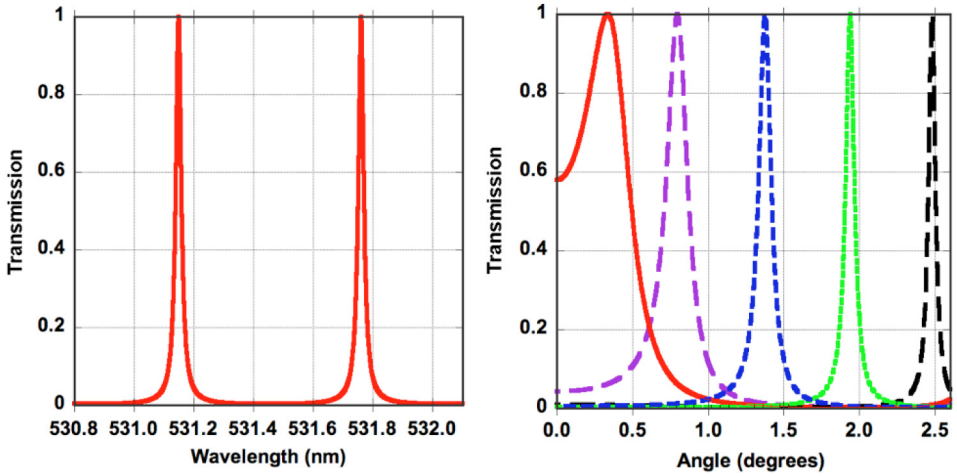

Fig. 1. Modeled transmission vs. wavelength at normal incidence (left) and transmission vs. angle of an etalon at multiple wavelengths (right) showing the dependence of these parameters.

Although etalons are capable of very high wavelength resolution, in general, they only transmit a very narrow wavelength band at a time coinciding with the current optical path length and angle of incidence (AOI). A key measure of etalon performance is the *finesse*, the ratio of the free spectral range (FSR) to the full-width at half-maximum (FWHM) transmission bandwidth [4]. A narrower filter (with the same free spectral range) rejects more out of band light. This means that as the resolving power (and finesse) are increased, more light is required to make a narrow-band measurement. In present systems, the light that is reflected is lost and only a very narrow band of light is measured. Scanning allows for the pass-band of the light to be changed but only one passband can be measured at any given time. This means that you need optical power (or integration time) to increase as the filter narrows so improving the resolution comes at the price of optical efficiency. Another common usage is to send a non-collimated beam through an etalon, which yields a well-known ring pattern and passes different wavelengths at different angles but is equally lossy. In contrast, a grating spectrometer splits the light of multiple wavelengths into different angles. This yields simultaneous wavelength measurements but with lower resolution (and generally high loss.) Another technology that has seen recent success is the Virtually Imaged Phased Array [5, 6] (VIPA). A VIPA can suffer from some of the same problems as gratings because the light is split into multiple orders and there is insertion loss in getting the light into the VIPA. The most desirable spectrometer is one that has simultaneous, continuous wavelength coverage like a grating spectrometer but maintains the resolution and luminosity of an etalon. In this paper, we demonstrate a novel optical scheme that achieves simultaneous (though not continuous) wavelength channels and maintains the resolution and luminosity of the etalon.

2. Design concept

Our novel spectrometer concept preserves the strengths of a Fabry-Perot etalon while improving on its main weakness – that it does not have parallel wavelength channels. We demonstrate a method to optically recirculate the light reflected from the etalon back through the same etalon at new angles. We create an etalon spectrometer based on angular dispersion without moving parts and without losing the light that is not initially transmitted. The only other configuration known to the authors that offers similar functionality is described by Jennings and Boyle [7]. Our system is simpler, more compact and designed for shorter wavelengths. The light transmitted at different angles can be separated using a transform lens to focus each angle onto a unique spot in the focal plane. Figure 2 shows an optical design

#249469 Received 3 Sep 2015; revised 2 Nov 2015; accepted 3 Nov 2015; published 6 Nov 2015
© 2015 OSA

that allows for angle-tuned transmission of an etalon. The diagram illustrates that by changing the distance of the input source relative to the optical axis, the AOI changes and therefore the transmission wavelength following Fig. 1.

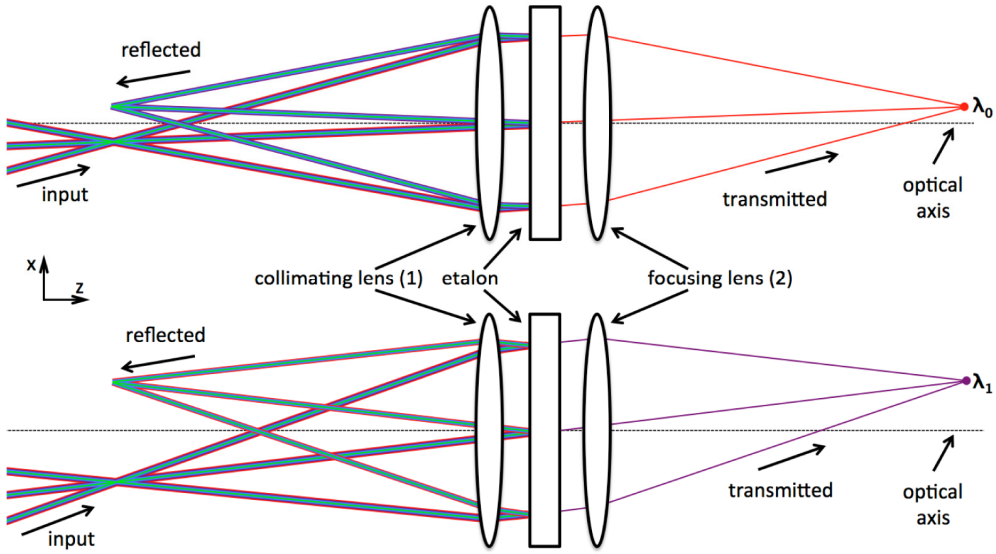

Fig. 2. Conceptual drawing of angle-dependent etalon transmission in a relevant optical configuration. Light of several wavelengths, shown here as red, purple, blue and green, enters from the left, is collimated and is incident on the etalon. In the top drawing, red light is transmitted and the remaining colors are reflected back to the left. In the bottom drawing, the input source focal spot is farther from the optical axis so after collimation it is incident on the etalon at a larger angle. In this configuration, the purple light is transmitted and the remaining light reflected.

Our optical design takes the light rejected by the initial etalon reflection and redirects it back to the etalon at a higher AOI. The light reflected the second time is reflected again at a further increased AOI and this process is repeated until the light has all dissipated. Figure 3 shows how this is accomplished.

The angular step-size between wavelengths is exaggerated in the illustration to avoid confusion but the angles can be spaced closely, limited only by the input beam spot size, the gap between the retro-reflecting mirrors (see Eq. (2) below) and optical aberrations. The light will continue to recirculate at ever increasing angles until no light remains or the beam gets clipped by the outer edge of the optics. As shown, each wavelength is imaged to a unique spot in the focal plane to the right of the etalon. These could be measured with a detector array or coupled into individual optical fibers for example.

#249469 Received 3 Sep 2015; revised 2 Nov 2015; accepted 3 Nov 2015; published 6 Nov 2015
© 2015 OSA

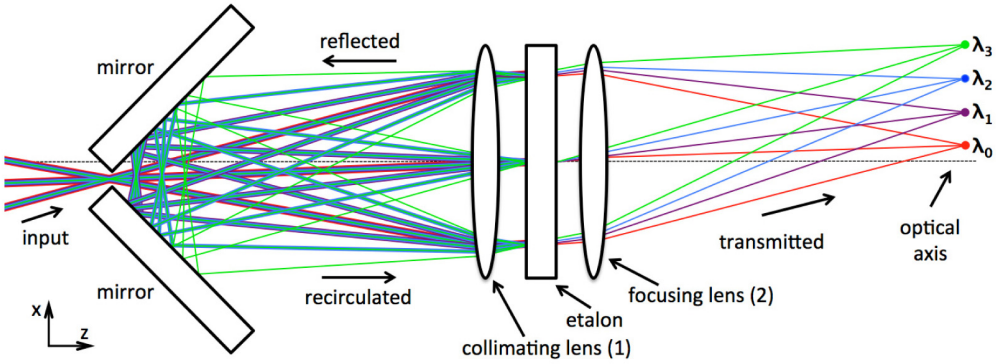

Fig. 3. Conceptual drawing of the novel recirculating etalon spectrometer. As in Fig. 2, a beam of light containing several wavelengths shines from the left, entering the spectrometer via a slit between two mirrors at ± 45° relative to the optical axis. The light is collimated and hits the etalon. The red light is transmitted and focused on the right focal plane. Purple, blue and green light are reflected back to the left, focused by the collimating lens, hits the top mirror, comes to a focus, hits the bottom mirror and then re-enters the system from the left at a virtual image point farther from the optical axis than the first pass. The light is then re-collimated and hits the etalon. Now the purple light is transmitted and focused on the right focal plane. The blue and green light is reflected back to the left and repeats the process with a virtual image point even farther from the optical axis than the second pass. With each successive pass, the beam is incident on the etalon at a higher angle and a different wavelength is transmitted.

3. Prototype demonstration and theory

We have built a proof-of-concept version of the recirculating etalon spectrometer (RES). The experimental set-up is shown in Fig. 4. For this demonstration we used aspheric lenses and dielectric coated mirrors. We used a PZT air-gapped etalon (Queensgate, Inc) that at 532 nm wavelength has a Free Spectral Range of 600 pm (Air-gap is 236 microns), a finesse of ~27 and a FWHM bandpass width of ~23 pm. We monitor the laser wavelength with a commercial wavelength meter to compare the results with the RES.

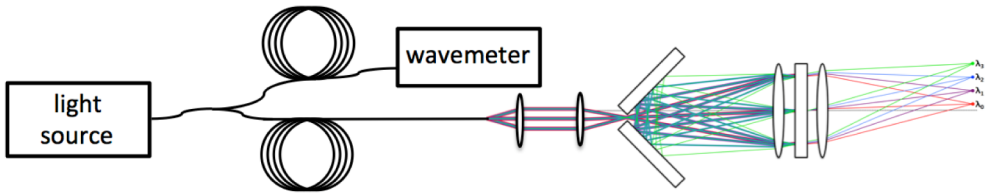

Fig. 4. Diagram of test set-up showing a fiber-coupled light source being analyzed by a commercial wavelength measurement system and by our novel apparatus.

We initially tested the recirculating optics concept (as shown in Fig. 4) with a multi-mode-fiber-coupled green LED. This tested the recirculating performance independent of wavelength and gave us insight into the alignment and round-trip loss of the system. (The loss is significant for this prototype and improvements will be discussed later.) This was successfully demonstrated and results are shown in Fig. 5. Alignment of the system is important for optimal performance. The two most important factors are getting the input light focused right at the slit between the two recirculating mirrors and adjusting the collimating lens for optimal collimation. In practice, manual 3-D linear translation stages on the input lens and the collimator are sufficient. Using the LED (or any broad wavelength source) to visualize all the channels simultaneously simplifies alignment because all the spots can be brought into focus together. Our optical model of this configuration shows the collimating lens can be off by as much as ± 0.28 mm before the channels bleed into one another. Tighter alignment is required for smaller angle separations, however the alignment tolerance is

#249469 Received 3 Sep 2015; revised 2 Nov 2015; accepted 3 Nov 2015; published 6 Nov 2015
© 2015 OSA

practical. After demonstrating the recirculation technique with the broad-band source, we then used a frequency-doubled 1062 nm DFB diode laser producing 531 nm single-mode-fiber-coupled output. This yields a single spatial mode, wavelength tunable, narrow spectrum light source. The laser source was tuned to different wavelengths, which were sorted into distinct channels shown in Fig. 6. No changes were made to the RES while the laser wavelength was tuned. This demonstrates the essentials of a wavelength division multiplexing (WDM) system though the device can be calibrated for use as a spectrometer to determine an unknown wavelength.

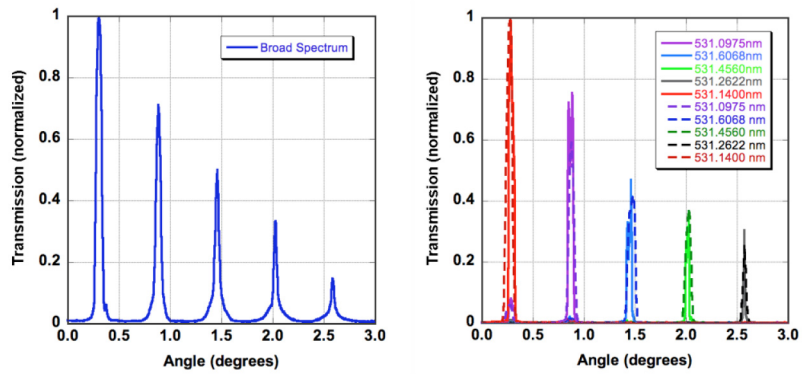

Fig. 5. This is a graph that shows the output of the spectrometer with (left) a broad spectral input and (right) at 5 different wavelengths (solid lines) with the modeled results for the same wavelengths (dashed lines).

We used a ray-tracing program (TracePro®) to model the theoretical performance of the RES and compare it to the measured data. (TracePro does not calculate interference so the etalon characteristics were imported.) We measured the etalon performance characteristics and used a matching MathCad® model to program the filter response in the TracePro model. We then modeled the RES prototype and the results are shown in Fig. 6 as dotted lines. In this prototype the overall light efficiency is limited by the loss in the etalon and a non-optimized optical design. Optimizing the design for low round trip loss will significantly increase the overall efficacy, but the basic functionality of the design is demonstrated with both the prototype and the model. Even for the current configuration, ~2.8 times more light is transmitted through this system in the 5 channels than is transmitted for the same etalon without the recirculated light. For many applications, this is a significant increase in photon efficiency and could be improved with lower round-trip loss and higher etalon transmission.

Using geometric optics and the paraxial approximation, it can be shown that the ith AOI, θ_i, is given by:

$$\theta_i = \frac{x_{offset}}{f_1}(1+2i); i = 0,1... \tag{1}$$

where x_{offset} is the distance the input beam is shifted from the optical axis(see axis in Fig. 3), f_1 is the collimating lens focal length and i is the number of recirculations the beam has made through the optics. To avoid clipping losses on the input and during the initial recirculation, geometry yields the condition:

$$2x_{offset} \geq slitwidth \geq w_0 \tag{2}$$

where w_0 is the incoming focused spot diameter, and the slit width is the distance between the two retro-reflecting mirror edges. (This assumes the mirror coating comes right to the edge of

#249469 Received 3 Sep 2015; revised 2 Nov 2015; accepted 3 Nov 2015; published 6 Nov 2015
© 2015 OSA

the mirror. In practice this may not be true and that edge effect would need to be accounted for.) The position of the ith transmitted spot, x_i', in the focal plane is given by:

$$x_i' = -\left(\frac{f_2}{f_1}\right)(1+2i)\,x_{offset}\,;\, i = 0,1... \tag{3}$$

where f_2 is the focusing lens focal length. The optical axis is normal to the etalon and passes through the center of lens 1 and we assume lens 1 & 2 have the same optical axis. It can be shown by sequentially tracing the optical path, the energy at a given wavelength of the nth spot in the image plane, $E_n(\lambda)$, can be represented by:

$$E_n(\lambda) = \left\{ \begin{array}{l} E_{input} T_{SP} (T_{RT})^n T_E(\theta_n, \lambda); n = 0 \\ E_{input} T_{SP} (T_{RT})^n \left[\prod_{i=0}^{n-1} 1 - T_E(\theta_i, \lambda) - \mathrm{A}_E \right] T_E(\theta_n, \lambda); n > 0 \end{array} \right\} \tag{4}$$

where E_{input} is the energy entering the spectrometer, T_{SP} is the single-pass transmission through the collimating and focusing lenses, T_{RT} is the round-trip transmission for 1 iteration through the recirculation optics, $T_E(\theta,\lambda)$ is the etalon transmission (given by the etalon equation, e.g. Hecht [4]), A_E is the etalon loss due to absorption and scattering and λ is the wavelength. From Eq. (4), it is clear that in order to maximize E_n for large n, the round trip loss and etalon loss must be minimized. If we use achievable numbers for the terms in Eq. (4), (e.g. - T_{SP} = 99%, T_{RT} = 99%, $T_E(\theta,\lambda)$ = 95%, A_E = 3%) we get ~80% transmission for the 5th spot. If we assume lower values, (e.g. - T_{SP} = 98%, T_{RT} = 98%, $T_E(\theta,\lambda)$ = 90%, A_E = 6%), we get ~60% transmission for the 5th spot. The surface quality on the recirculating mirrors does not need to be extremely good because only a small area is being used because the beam is at a near focus. High reflectivity is important as can be seen above but commercial mirrors are available with much better than 99% reflectivity. This means the etalon transmission and absorption are critical factors in a low loss system.

4. Applications and design considerations

One important application for the RES is atomic and molecular spectroscopy in photon-starved scenarios such as remote sensing instruments [8–10]. To illustrate the utility, we configured the RES for simultaneous measurement of the sodium D1 and D2 lines whose separation is 0.6 nm. The experimental arrangement is the same as that shown in Fig. 4 with the light source being a Philips 234047-SOX-E18 low-pressure sodium light bulb coupled into a multi-spatial mode fiber and the wavemeter being a scanning grating spectrometer (ANDO Model AQ6315B). The etalon air-gap spacing is 236 microns (FSR at 589 nm = 735 pm). The etalon air-gap spacing and lens offset were adjusted so that, with recirculation, both the D1 and D2 lines are resonant and transmit through the etalon simultaneously (i.e. within the recirculation time). Figure 6 compares the spectra of the sodium lamp from the grating spectrometer (left) and the Recirculating Etalon Spectrometer – (right). In a traditional etalon set-up, we would see either D2 at one angle or D1 at another angle but this demonstration shows both lines simultaneously illustrating the potential improved photon efficiency.

#249469 Received 3 Sep 2015; revised 2 Nov 2015; accepted 3 Nov 2015; published 6 Nov 2015
© 2015 OSA

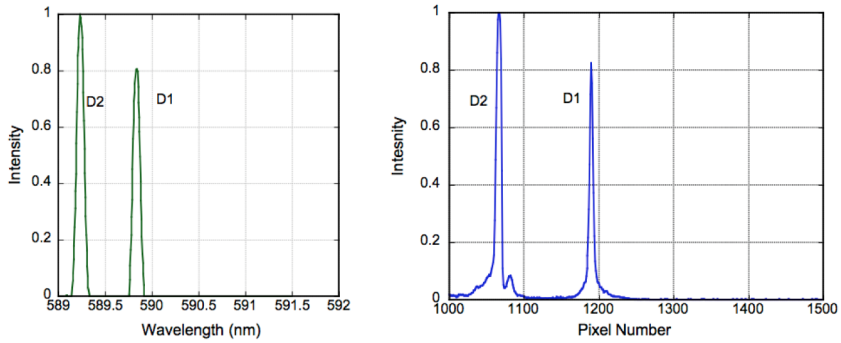

Fig. 6. Comparison of sodium lamp spectra from (left) conventional scanning grating spectrometer and (right) Recirculating Etalon Spectrometer

We have built a prototype of a recirculating etalon spectrometer and demonstrated its basic functionality and utility. Further development is required to optimize the design and realize its full potential. We built the current prototype around a PZT etalon because it was the highest finesse etalon we had on hand. We used off-the-shelf parts to demonstrate the basic function. There are a number of improvements that can be made as well as a number of different optical configurations to potentially achieve similar results. In the current implementation, we used all spherical (or aspherical) lenses. However, because all the wavelength dispersion happens in a single plane, the lenses could be replaced with cylindrical lenses allowing other functions to occur in the orthogonal axis (e.g - a grating separating wavelengths in the y-axis would enable use of the RES over many free-spectral ranges without ambiguity.) In general there is a great deal of freedom in the selection of the lens design that would need to be optimized for a specific application. A primary factor is the etendue of the system. The field of view (FOV) of an etalon is maximum at normal incidence and decreases at higher angles (illustrated in Fig. 1) so the lens design, aperture and spatial mode quality will need to match the FOV of the etalon at the largest AOI used to maintain good transmission at those angles. As demonstrated in the prototype, this can be achieved but system performance for a given application will depend on the correct trade between the aperture, f# of the collimator and aberrations and walk off from repeated recirculations of the beam. Also the collimating lens and focusing lens can be different so the focusing lens can be optimized for the focal plane requirements while the collimating lens can be designed to optimize recirculation performance.

One feature of this recirculating configuration should be noted: the increase in AOI in successive round trips is constant but because the wavelength transmission peak is not a linear function of AOI for an etalon, the wavelength step size is not constant for each successive round trip. However, (aside from the usual etalon ambiguity resulting from the free spectral range) there is a one-to-one mapping of angle to wavelength so the RES can be calibrated to measure the spectra accurately but the mapping function is more complicated due to the iterative nature of the measurement. The free spectral range ambiguity inherent to etalons can be resolved by passing the light through a band-pass filter that corresponds to the range of interest.

Another feature of the current apparatus is that light is never incident on the etalon at exactly normal incidence. We have looked at a variant of the current design where the two mirrors are replaced with a saw-tooth retro-reflecting array. This is shown in Fig. 7. In this variation, normal incidence can be achieved as well as other interesting features at the expense of a slightly more complicated arrangement. We have also modeled a cats-eye reflector array that could operate in a similar fashion. In this arrangement, it is possible to start at higher angles and work toward normal incidence. The reflector array shown is rather

#249469 Received 3 Sep 2015; revised 2 Nov 2015; accepted 3 Nov 2015; published 6 Nov 2015
© 2015 OSA

large for illustrative purposes but as with the original design, the angular step size can be quite small – in this case limited by the manufacturing of the reflector.

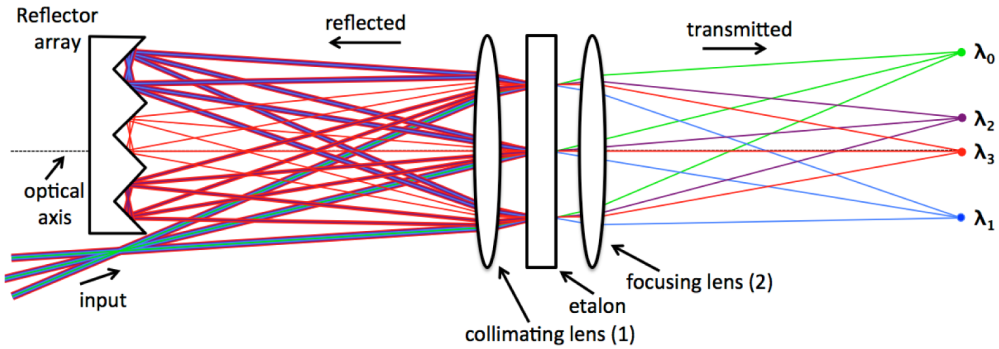

Fig. 7. Diagram of saw-tooth retro-reflector. In this figure, an array of reflectors replace the bulk mirrors so that each recirculation has its own retroreflector.

Our prototype has demonstrated the use of completely fixed optical components but it could be advantageous to allow etalon-scanning to optimize the transmission of one or more wavelengths. In its current arrangement the wavelength resolution demonstrated is rather granular. The wavelength coverage is not complete, and adjacent wavelength channels have a minimal distance (subject to the restriction listed in Eq. (2), which ultimately limits total throughput for broadband spectra. Improved wavelength coverage is easily accomplished by adjusting the initial beam displacement.

5. Conclusions

Our novel spectrometer has the potential to improve the performance of many optical spectral measurements. It will potentially provide extremely high wavelength resolution spectral measurements for very weak signals, which could enable several applications. Additional applications include lidar instruments requiring spectral resolution such as trace-gas differential absorption spectroscopy, measurement of Doppler shifts for wind and wavelength division multiplexing and de-multiplexing for optical communication and laser altimetry.

#249469 Received 3 Sep 2015; revised 2 Nov 2015; accepted 3 Nov 2015; published 6 Nov 2015
© 2015 OSA